Quantum algorithms for generator coordinate methods

Muqing Zheng, ^{1,2} Bo Peng, ² Nathan Wiebe, ^{2,3} Ang Li , ² Xiu Yang , ¹ and Karol Kowalski^{2,*}

¹Lehigh University, Bethlehem, Pennsylvania 18015, USA

²Pacific Northwest National Laboratory, Richland, Washington 99354, USA

³University of Toronto, Toronto, Ontario M5G 1Z8, Canada

(Received 28 December 2022; accepted 29 April 2023; published 28 June 2023)

This paper discusses quantum algorithms for the generator coordinate method (GCM) that can be used to benchmark molecular systems. The GCM formalism defined by exponential operators with exponents defined through generators of the fermionic U(N) Lie algebra (Thouless theorem) offers a possibility of probing large subspaces using low-depth quantum circuits. In the present study, we illustrate the performance of the quantum algorithm for constructing a discretized form of the Hill-Wheeler equation for ground- and excited-state energies. We also generalize the standard GCM formulation to multiproduct extension that when collective paths are properly probed can systematically introduce higher rank effects and provide elementary mechanisms for symmetry purification when generator states break the spatial or spin symmetries. The GCM quantum algorithms also can be viewed as an alternative to existing variational quantum eigensolvers, where multistep classical optimization algorithms are replaced by a single-step procedure for solving the Hill-Wheeler eigenvalue problem.

DOI: 10.1103/PhysRevResearch.5.023200

I. INTRODUCTION

The rapid development of quantum technologies and quantum algorithms addresses long-standing computational challenges of many-body physics and quantum chemistry. While the primary target is to overcome exponential growth in complexity associated with approaching the exact limit in the simulations, the possibility of identifying physically meaningful solutions to problems of interest is equally important. Although Quantum Phase Estimation algorithms [1–7] have been designed in a way that adequately addresses both of these issues, their applicability is currently limited by the necessity of using complex quantum circuits with corresponding depths that preclude its practical applications on existing quantum computing platforms, dominated by Noisy Intermediate-Scale Quantum (NISQ) devices. Instead, hybrid algorithms such as various Variational Quantum Eigensolvers (VQEs) [8–26] are currently being intensively tested on NISQ quantum computers to characterize the properties of correlated quantum systems. In this effort, in many aspects, the VQE formulations, for example, based on the unitary coupledcluster (UCC) [27–31] representation of the wave function, mirror the standard conventional formulations of CC theory, where a large number of excitations are included in the cluster operator and simultaneously optimized in the iterative process. This algorithm leads to another set of challenges associated with the potential problems with the convergence of iterative processes (commonly referred to as the barren

Published by the American Physical Society under the terms of the Creative Commons Attribution 4.0 International license. Further distribution of this work must maintain attribution to the author(s) and the published article's title, journal citation, and DOI.

minimum problem) and representation of UCC ansatz on quantum registers, which may result in long Trotter-like products of exponential operators defined by multiqubit gates. Although several strategies mitigating these problems have recently been proposed, utilizing VQE-UCC formulations and extending these methods beyond specific system-size limits may be challenging and require reformulation of the quantum many-body problem into recently introduced quantum flow equations [32], where large subspaces of Hilbert space can be sampled through the constant-depth small-dimensionality coupled eigenproblems.

Instead, in this paper we explore the applicability of the Generator Coordinate Method (GCM) [33–39] as an alternative to popular VQE formulations. The main difference with the VQE method is that the GCM method avoids highly nonlinear parametrization of the wave function and provides an efficient mean for direct extension of the probed subspaces. Additionally, it offers an efficient utilization of ansatzes represented by low-depth quantum circuits.

The GCM method was one of the first attempts to combine two distinct aspects of many-body theories: independent-particle models and theories describing collective phenomena, where the approximate eigenstates $|\Psi_{GCM}\rangle$ of the Hamiltonian H are expressed using a family of N-body wave functions $|\Phi(\mathbf{q})\rangle$,

$$|\Psi_{\text{GCM}}\rangle = \int d\mathbf{q} |\Phi(\mathbf{q})\rangle f(\mathbf{q}),$$
 (1)

where \mathbf{q} is a set of collective variables that describe correlation effects in many-body systems, and, usually, the corresponding $|\Phi(\mathbf{q})\rangle$ is represented as a complicated linear combination of Slater determinants. The scalar $f(\mathbf{q})$ is referred to as the weight function. The advantage of the GCM approach is obtaining ground states and classes of excited states described by the chosen set of generator coordinates. In general, in

^{*}karol.kowalski@pnnl.gov

the analogy to the coherent state representation [40,41], the family $|\Phi(\mathbf{q})\rangle$ forms an overcomplete basis. Upon substituting (1) into the Schrödinger equation one gets the so-called Hill-Wheeler integral equations for unknown $f(\mathbf{q})$ coefficients

$$\int d\mathbf{q}' [\mathbf{H}(\mathbf{q}, \mathbf{q}') - E\mathbf{S}(\mathbf{q}, \mathbf{q}')] f(\mathbf{q}') = 0,$$
 (2)

where the integral kernels **H** and **S** are defined as

$$\mathbf{H}(\mathbf{q}, \mathbf{q}') = \langle \Phi(\mathbf{q}) | H | \Phi(\mathbf{q}') \rangle, \tag{3}$$

$$\mathbf{S}(\mathbf{q}, \mathbf{q}') = \langle \Phi(\mathbf{q}) | \Phi(\mathbf{q}') \rangle. \tag{4}$$

In typical applications, the Hill-Wheeler equation is usually solved numerically by discretization, which transforms integral equation (3) into an algebraic eigenvalue problem.

There are two categories of GCM formulations in applications to many-body quantum systems. The first category's purpose is to restore broken symmetries of the $|\Phi(\mathbf{q})\rangle$ states. For example, Bardeen-Cooper-Schrieffer states are not eigenstates of the particle number operator N. In this case, the properties of $f(\mathbf{q}_k)$ coefficients are determined by the properties of the symmetry (projection) operators (e.g., particle number projection operator). In the second category of GCM formulations, the unknown weight function is optimized to capture correlation effects encoded in generator coordinates. However, designing an adequate grid or path to probe the Hill-Wheeler equation is a rather empirical procedure that requires much intuition and prior knowledge of the sought-after many-body system.

The appealing feature of the GCM method, especially from the point of possible quantum computing applications, is the possibility of combining low-depth representations of $|\Phi(\mathbf{q})\rangle$ functions with simple, one-step optimization conditions for weight function. In this approach, the role of quantum computing is to map a discrete number of states $\{|\Phi(\mathbf{q}_p)\rangle\}_{n=1}^M$ to a quantum register and to evaluate matrix elements for Hamiltonian and overlap matrices [Eqs. (3) and (4)]. In contrast, solving a generalized eigenvalue problem in a discrete basis representation takes place only once on a classical computer, avoiding multiple instances of quantum-classical communication as in the VQE formalism. In the discussed formalism, we follow an "algebraic" GCM formulation discussed by Fukutome in Ref. [42], extend the standard GCM to multiproduct exponential formulas, and provide an algorithm for sampling coordinate space in a way that provides selective approaching classes of excited Slater determinants. In this context, the multiproduct GCM formulation alleviates some problems associated with the usage of high fidelity of Trotter-type expansions.

We demonstrate the performance of the quantum GCM algorithm on the example of the H4 benchmark system in various configurations. We show that one can recover a high level of accuracy in both weakly and strongly correlated regimes using $|\Phi(\mathbf{q})\rangle$'s that use the manifold of single excitations [or U(N) Lie algebra generators]. The obtained level of accuracy is similar to the one obtained with the advanced VQE formulations.

II. THEORY

The GCM was initially introduced to describe collective effects in nuclei [33,36,39,43]. Fukutome in his seminal paper [42] considered the GCM from the Lie-algebra theoretical standpoint. We use that language throughout this paper. Let us assume that the fermion system is described by annihilation and creation operators a_p and a_q^{\dagger} that satisfy the following set of anticommutation relations:

$$[a_p, a_q]_+ = [a_p^{\dagger}, a_q^{\dagger}]_+ = 0, \quad [a_p, a_q^{\dagger}]_+ = \delta_{pq}.$$
 (5)

As discussed in Ref. [42] there are several fermion algebras including U(N), SO(2N), and SO(2N+1) Lie algebras, and Clifford algebras that can be used to characterize approximate many-body wave functions (here N stands for the number of single-particle states). These algebras can be defined by the following set of operators:

$$E_q^p = a_p^{\dagger} a_q - \frac{1}{2} \delta_{pq}, \ E_{pq} = a_p a_q, \ E^{pq} = a_p^{\dagger} a_q^{\dagger}.$$
 (6)

For example,

$$U(N)$$
: $\{E_q^p\}$,
 $SO(2N)$: $\{E_q^p, E_{pq}, E^{pq}\}$,
 $SO(2N+1)$: $\{a_p, a_q^{\dagger}, E_q^p, E_{pq}, E^{pq}\}$.

The U(N) algebra is the only algebra where particle number operator commutes with all operators belonging to U(N) algebra. The Lie algebras listed above generate canonical transformations on the fermion space and provide theoretical language to construct independent particle and quasiparticle models such as Hartree-Fock or Hartree-Fock-Bogoliubov formalisms as well as higher-order formulations such as configuration interaction or coupled cluster theories (more details can be found in Refs. [36,42,44–46]). Recently, many-body algebras have attracted much attention in the context of quantum computing [47–49].

Let us focus attention on the U(N) algebra. By $\Gamma(\mathbf{Z})$ we designate an anti-Hermitian operator defined as

$$\Gamma(\mathbf{Z}) = \sum_{p,q} z_{pq} E_q^p = \sum_{p,q} z_{pq} a_p^{\dagger} a_q \; , \; \; z_{qp}^{\star} = -z_{pq}, \quad (7)$$

where **Z** can be viewed as an anti-Hermitian matrix $[z_{pq}]$ where $z_{qp}^{\star} = -z_{pq}$ or set of indexed parameter $\{z_{pq}\}$ satisfying $z_{qp}^{\star} = -z_{pq}$. Canonical transformation $U(\mathbf{Z})$ generated by $\Gamma(\mathbf{Z})$ takes the form

$$U(\mathbf{Z}) = e^{\Gamma(\mathbf{Z})}. (8)$$

Standard canonical Thouless transformation of the Hartree-Fock (HF) determinant $|\Phi\rangle$ can be obtained by acting with $U(\mathbf{Z})$ onto $|\Phi\rangle$:

$$|\Phi(\mathbf{Z})\rangle = U(\mathbf{Z})|\Phi\rangle = e^{\Gamma(\mathbf{Z})}|\Phi\rangle.$$
 (9)

The standard unitary CC model with singles (UCCS) is a special case of (9) where $z_{ij} = z_{ab} = 0$, where i, j, ... and a, b, ... correspond to spin-orbital indices occupied and unoccupied in the Slater determinant $|\Phi\rangle$ (where **Z** can be identified with the set of elements $\{z_{ia}\}$). In comparison to $|\Phi\rangle$, $|\Phi(\mathbf{Z})\rangle$ can contain certain classes of correlation effects (that are **Z** dependent); it can contain elements of symmetry breaking and effects responsible for the appearance of HF instabilities (for the discussion of the role of the Thouless theorem in identifying the instabilities of HF solutions; see Appendix A).

The parametrized states (9) can be viewed as a nonorthogonal (in general overcomplete) basis in the Hilbert space. The generator coordinate method utilizes this fact by representing the wave function in the form

$$|\Psi_{\text{GCM}}\rangle = \int d\mathbf{Z} |\Phi(\mathbf{Z})\rangle f(\mathbf{Z}),$$
 (10)

where collective variables \mathbf{q} of Eq. (1) are now identified with \mathbf{Z} matrix:

$$\mathbf{q} \to \mathbf{Z}$$
. (11)

A typical way for solving Hill-Wheeler equations (2) is through discretization of the **Z** domain. Let us introduce a set of the **Z** points $Q = \{\mathbf{Z}_i\}_{i=1}^M$; then Eq. (2) takes the form of nonorthogonal eigenvalue problem

$$\mathbf{Hf} = E\mathbf{Sf},\tag{12}$$

where **H** and **S** ($M \times M$ matrices) and **f** (M-dimensional vector) are defined as follows:

$$\mathbf{H}_{pq} = \langle \Phi(\mathbf{Z}_p) | H | \Phi(\mathbf{Z}_q) \rangle, \tag{13}$$

$$\mathbf{S}_{pq} = \langle \Phi(\mathbf{Z}_p) | \Phi(\mathbf{Z}_q) \rangle, \tag{14}$$

$$\mathbf{f}_n = f(\mathbf{Z}_n). \tag{15}$$

Using this form of discretization, the optimal form of the wave function (we assume the ground-state wave function in this paper) is given by the expansion

$$|\Psi_{\text{GCM}}\rangle \simeq \sum_{p=1}^{M} \mathbf{f}_{p} e^{\Gamma(\mathbf{Z}_{p})} |\Phi\rangle,$$
 (16)

which is reminiscent of recently discussed nonorthogonal variational approaches discussed in the context of quantum computing [15], If M is equal for a given basis set to a dimension of the full configuration interaction (FCI) problem (for a given spin and spatial symmetry) and $e^{\Gamma(\mathbf{Z}_p)}|\Phi\rangle$ are linearly independent, then the expansion (16) with optimized f_i coefficients describes the exact electronic wave function. In the following part of the paper, Eq. (12) is used to calculate ground- and excited-state energies.

III. MULTIPRODUCT EXTENSION OF THE GENERATOR COORDINATE FORMALISM

A possible extension of the GCM expansion given by Eq. (10) can be provided by the expansion involving multiple products (the product GCM formalism, abbreviated as $PGCM^{(k)}$) of k exponential operators (which is inspired by a recent progress in the development of dynamical GCM methods [39,43,50–52]). For example, one can introduce the following expansion:

$$|\Psi_{\text{PGCM}}^{(k)}\rangle = \int d\mathbf{Z}(1) \dots d\mathbf{Z}(k) \times |\Phi^{(k)}(\mathbf{Z}(1), \dots, \mathbf{Z}(k))\rangle f(\mathbf{Z}(1), \dots, \mathbf{Z}(k)), \tag{17}$$

where

$$|\Phi^{(k)}(\mathbf{Z}(1),\ldots,\mathbf{Z}(k))\rangle = e^{\Gamma(\mathbf{Z}(k))}\cdots e^{\Gamma(\mathbf{Z}(1))}|\Phi\rangle.$$
 (18)

In the above representation, $\Gamma(\mathbf{Z}(i))$ can belong to various Lie algebras. In the following we will focus on the case where all $\Gamma(\mathbf{Z}(i))$'s (i = 1, ..., k) belong to the same U(N) Lie algebra:

$$\Gamma(\mathbf{Z}(i)) = \sum_{pq} z_{pq}(i) E_q^p, \ z_{qp}(i)^* = -z_{pq}(i).$$
 (19)

In fact, the PGCM formula may be viewed as a special case of the GCM where

$$\mathbf{q} \to \mathbf{Z}(1) \times \ldots \times \mathbf{Z}(k)$$
. (20)

We will demonstrate that the U(N) case of PGCM lends itself to an efficient way of representing higher-rank excitations in quantum computing. In particular, this goal can be achieved by using a simple algorithm for discretization of $\mathbf{Z}(i)$ domains in the GCM method. In particular, we can show that PGCM^(k) can be used to approximate 2k-tuple excitations in the configuration-interaction-type expansion.

Let us focus on the specific case when k=2 (i.e., the PGCM⁽²⁾formalism). In this case we will represent the $|\Psi_{PGCM}^{(2)}\rangle$ wave function, given by the following formulas:

$$\left|\Psi_{\text{PGFM}}^{(2)}\right\rangle = \int d\mathbf{Z}(1)d\mathbf{Z}(2)|\Phi^{(2)}(\mathbf{Z}(1),\mathbf{Z}(2))\rangle$$

$$\times f(\mathbf{Z}(1),\mathbf{Z}(2)) \tag{21}$$

and

$$|\Phi^{(2)}(\mathbf{Z}(1), \mathbf{Z}(2))\rangle = e^{\Gamma(\mathbf{Z}(2))} e^{\Gamma(\mathbf{Z}(1))} |\Phi\rangle. \tag{22}$$

The GCM algorithm can be adapted easily for the product representation of the trial wave functions. Now the discretization of the problem, in analogy to Eq. (12), involves a Q set defined as $Q = \{\mathbf{Z}_I\}_I$, where $\mathbf{Z}_I = \mathbf{Z}(1)_p \times \mathbf{Z}(2)_q$, where we use composite index I = (p,q). Controllable sampling algorithms of the subspaces of the Hilbert space corresponding to higher-rank excitations with the PGCM formalism based on the U(N) algebras requires careful selection of the sampling points, which will be discussed in the following section in the context of PGCM⁽²⁾ method applications to the H4 system.

IV. H4 MODEL: CHOICE OF GCM SAMPLING POINTS

We use the H4 model of Ref. [53] as a benchmark system, which has been used in studies of strong correlation effects in many-body systems, for example, in the analysis of multireference coupled-cluster theories, [54] and intruder-state problems, stability of solutions of Hartree-Fock equations [55], and quantum computing algorithms [56]. The system's geometry can be defined by a single parameter α (see Fig. 1). For $\alpha = 0.5$, the H4 model corresponds to a linear chain of hydrogen atoms with distances between adjacent hydrogen atoms equal to 2.0 a.u.; for $\alpha = 0.005$, the system is almost in a square configuration. The main difference between $\alpha = 0.5$ and $\alpha = 0.005$ H4 models is in the structure of the corresponding ground-state wave function. While for $\alpha = 0.5$, the ground-state wave function is dominated by the restricted Hartree-Fock (RHF) determinant, for $\alpha = 0.005$, the ground state is quasidegenerate. The contribution of the RHF Slater determinant is almost the same as the doubly excited configuration where two electrons from the highest

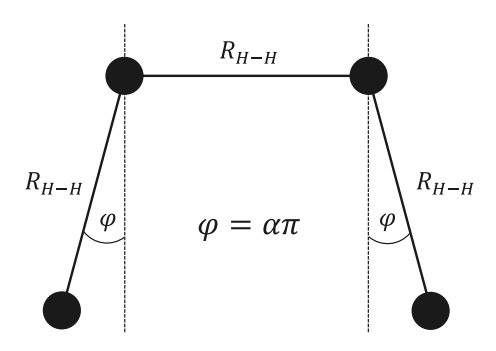


FIG. 1. Schematic representation of the H4 model system. The geometry of the system is defined by a single parameter α . The distance between contiguous hydrogen atoms is set to $R_{H-H} = 2.0$ a.u.

occupied orbital are promoted to the lowest-lying virtual orbital. The spin-orbital numbering scheme is shown in Fig. 2. In the PGCM⁽²⁾ formalism for H4, we will adopt the following sampling scheme, where the choice of the cluster operators is consistent with analyzing HF equation stability conditions based on the Thouless theorem [44,58–60]:

$$|R_0\rangle = |\Phi\rangle, \tag{23}$$

$$P(\pm)\langle \cdot, \cdot \rangle = \pm t_0 R_0 + \epsilon_0 \left[(a^{\dagger}a_2 + a^{\dagger}a_3) - (a^{\dagger}a_5 + a^{\dagger}a_3) \right] + \epsilon_0 \left[(a^{\dagger}a_3 + a^{\dagger}a_3) - (a^{\dagger}a_5 + a^{\dagger}a_3) \right] + \epsilon_0 \left[(a^{\dagger}a_3 + a^{\dagger}a_3) - (a^{\dagger}a_5 + a^{\dagger}a_3) \right] + \epsilon_0 \left[(a^{\dagger}a_3 + a^{\dagger}a_3) - (a^{\dagger}a_5 + a^{\dagger}a_3) \right] + \epsilon_0 \left[(a^{\dagger}a_3 + a^{\dagger}a_3) - (a^{\dagger}a_5 + a^{\dagger}a_3) \right] + \epsilon_0 \left[(a^{\dagger}a_3 + a^{\dagger}a_3) - (a^{\dagger}a_5 + a^{\dagger}a_3) \right] + \epsilon_0 \left[(a^{\dagger}a_3 + a^{\dagger}a_3) - (a^{\dagger}a_5 + a^{\dagger}a_3) \right] + \epsilon_0 \left[(a^{\dagger}a_3 + a^{\dagger}a_3) - (a^{\dagger}a_5 + a^{\dagger}a_3) \right] + \epsilon_0 \left[(a^{\dagger}a_3 + a^{\dagger}a_3) - (a^{\dagger}a_5 + a^{\dagger}a_3) \right] + \epsilon_0 \left[(a^{\dagger}a_3 + a^{\dagger}a_3) - (a^{\dagger}a_5 + a^{\dagger}a_3) \right] + \epsilon_0 \left[(a^{\dagger}a_3 + a^{\dagger}a_3) - (a^{\dagger}a_5 + a^{\dagger}a_3) \right] + \epsilon_0 \left[(a^{\dagger}a_3 + a^{\dagger}a_3) - (a^{\dagger}a_5 + a^{\dagger}a_3) \right] + \epsilon_0 \left[(a^{\dagger}a_3 + a^{\dagger}a_3) - (a^{\dagger}a_5 + a^{\dagger}a_3) \right] + \epsilon_0 \left[(a^{\dagger}a_3 + a^{\dagger}a_3) - (a^{\dagger}a_5 + a^{\dagger}a_3) \right] + \epsilon_0 \left[(a^{\dagger}a_3 + a^{\dagger}a_3) - (a^{\dagger}a_5 + a^{\dagger}a_3) \right] + \epsilon_0 \left[(a^{\dagger}a_3 + a^{\dagger}a_3) - (a^{\dagger}a_5 + a^{\dagger}a_3) \right] + \epsilon_0 \left[(a^{\dagger}a_3 + a^{\dagger}a_3) - (a^{\dagger}a_5 + a^{\dagger}a_3) \right] + \epsilon_0 \left[(a^{\dagger}a_3 + a^{\dagger}a_3) - (a^{\dagger}a_5 + a^{\dagger}a_3) \right] + \epsilon_0 \left[(a^{\dagger}a_3 + a^{\dagger}a_3) - (a^{\dagger}a_5 + a^{\dagger}a_3) \right] + \epsilon_0 \left[(a^{\dagger}a_3 + a^{\dagger}a_3) - (a^{\dagger}a_5 + a^{\dagger}a_3) \right] + \epsilon_0 \left[(a^{\dagger}a_3 + a^{\dagger}a_3) - (a^{\dagger}a_5 + a^{\dagger}a_3) \right] + \epsilon_0 \left[(a^{\dagger}a_3 + a^{\dagger}a_3) - (a^{\dagger}a_5 + a^{\dagger}a_3) \right] + \epsilon_0 \left[(a^{\dagger}a_3 + a^{\dagger}a_3) - (a^{\dagger}a_5 + a^{\dagger}a_3) \right] + \epsilon_0 \left[(a^{\dagger}a_3 + a^{\dagger}a_3) - (a^{\dagger}a_5 + a^{\dagger}a_3) \right] + \epsilon_0 \left[(a^{\dagger}a_3 + a^{\dagger}a_3) - (a^{\dagger}a_5 + a^{\dagger}a_3) \right] + \epsilon_0 \left[(a^{\dagger}a_3 + a^{\dagger}a_3) - (a^{\dagger}a_3 + a^{\dagger}a_3) \right] + \epsilon_0 \left[(a^{\dagger}a_3 + a^{\dagger}a_3) - (a^{\dagger}a_3 + a^{\dagger}a_3) \right] + \epsilon_0 \left[(a^{\dagger}a_3 + a^{\dagger}a_3) - (a^{\dagger}a_3 + a^{\dagger}a_3) \right] + \epsilon_0 \left[(a^{\dagger}a_3 + a^{\dagger}a_3) - (a^{\dagger}a_3 + a^{\dagger}a_3) \right] + \epsilon_0 \left[(a^{\dagger}a_3 + a^{\dagger}a_3) - (a^{\dagger}a_3 + a^{\dagger}a_3) \right] + \epsilon_0 \left[(a^{\dagger}a_3 + a^{\dagger}a_3) - (a^{\dagger}a_3 + a^{\dagger}a_3) \right] + \epsilon_0 \left[(a^{\dagger}a_3 + a^{\dagger}a_3) - (a^{\dagger}a_3 + a^{\dagger}a_3) \right] + \epsilon_0 \left[(a^{\dagger}a_3 + a^{\dagger}a_3) - (a^{\dagger}a_3 + a^{\dagger}a_3) \right] + \epsilon_0 \left[(a^{\dagger}a_3 + a^{\dagger}a_3) - (a^{\dagger}a_3 + a^{\dagger}a_3) \right] + \epsilon_0 \left[(a^{\dagger}a_3 + a^{\dagger}$$

$$|R_1^{(\pm)}(t_1)\rangle = e^{\pm t_1 R_1} |\Phi\rangle = e^{\pm t_1 [(a_5^{\dagger} a_2 + a_7^{\dagger} a_4) - (a_2^{\dagger} a_5 + a_4^{\dagger} a_7)]} |\Phi\rangle,$$
(24)

$$|R_2^{(\pm)}(t_2)\rangle = e^{\pm t_2 R_2} |\Phi\rangle = e^{\pm t_2 [(a_6^{\dagger} a_1 + a_8^{\dagger} a_3) - (a_1^{\dagger} a_6 + a_3^{\dagger} a_8)]} |\Phi\rangle,$$
(25)

$$|R_3^{(\pm)}(t_3)\rangle = e^{\pm t_3 R_3} |\Phi\rangle = e^{\pm t_3 [(a_6^{\dagger} a_2 + a_8^{\dagger} a_4) - (a_2^{\dagger} a_6 + a_4^{\dagger} a_8)]} |\Phi\rangle,$$
(26)

$$|R_4^{(\pm)}(t_4)\rangle = e^{\pm t_4 R_4} |\Phi\rangle = e^{\pm t_4 [(a_5^{\dagger} a_1 + a_7^{\dagger} a_3) - (a_1^{\dagger} a_5 + a_3^{\dagger} a_7)]} |\Phi\rangle, \tag{27}$$

$$|R_5(t_5)\rangle = e^{t_5 R_3} e^{t_5 R_4} |\Phi\rangle, \tag{28}$$

$$|R_6(t_6)\rangle = e^{t_6 R_4} e^{t_6 R_3} |\Phi\rangle,$$
 (29)

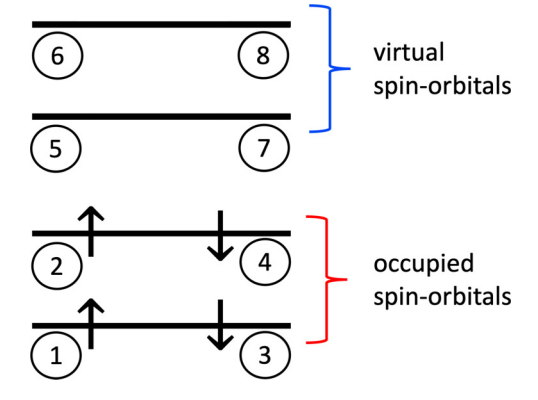


FIG. 2. Schematic representation of the orbital energies and the enumeration scheme for the corresponding spin orbitals for the H4 model in the STO-3G basis set [57]. Spin orbitals 1,2 and 3,4 correspond to occupied α and β spin orbitals, respectively, while spin orbitals 5,6 and 7,8 correspond to virtual α and β spin orbitals.

$$\begin{aligned} & \left| R_{2}^{(\pm)} R_{1}^{(\pm)}(t_{7}) \right\rangle \\ &= e^{\pm t_{7} R_{2}} e^{\pm t_{7} R_{1}} |\Phi\rangle \\ &= e^{\pm t_{7} [(a_{6}^{\dagger} a_{1} + a_{8}^{\dagger} a_{3}) - (a_{1}^{\dagger} a_{6} + a_{3}^{\dagger} a_{8})]} e^{\pm t_{7} [(a_{5}^{\dagger} a_{2} + a_{7}^{\dagger} a_{4}) - (a_{2}^{\dagger} a_{5} + a_{4}^{\dagger} a_{7})]} |\Phi\rangle. \end{aligned}$$

$$(30)$$

These sampling vectors can be naturally tied to the general form of the $|\Phi^{(2)}(\mathbf{Z}(1),\mathbf{Z}(2))\rangle$ basis given by Eq. (22). For example, $|R_0\rangle$ corresponds to $\mathbf{Z}(1) = \mathbf{Z}(2) = 0$. For $|R_1^{(+)}(t_1)\rangle$, $\mathbf{Z}(2) = 0$, and $z(1)_{52} = z(1)_{74} = -z(1)_{25} = -z(1)_{47} = t_1$ while remaining matrix elements are equal to zero, etc. Another advantage of using this form of sampling vectors is that their combinations provide a rudimentary (yet not exact) mechanism for eliminating symmetry impurities when R_i operators break the symmetry of the reference state $|\Phi\rangle$. For example, if in general $R_1^{(\pm)}(t_1)$ the operator is expressed in terms of excitations that can produce broken symmetry state when acting on the reference function, and then this singly excited impurity (or instability) is eliminated by taking a combination of $|R_1^{(+)}\rangle + |R_1^{(-)}\rangle$ states,

$$|R_1^{(+)}(t_1)\rangle + |R_1^{(-)}(t_1)\rangle = (e^{t_1R_1} + e^{-t_1R_1})|\Phi\rangle$$

$$= \left(2 + t_1^2 R_1^2 + \frac{2}{4!} t_1^4 R_1^4 + \dots\right)|\Phi\rangle, \tag{31}$$

where linear "impurities" are eliminated. These combinations also can allow us to selectively approach doubly excited configurations, or using combinations of $|R_2^{(\pm)}R_1^{(\pm)}(t_7)\rangle$, quadruply excited ones using manifold of single excitations and very simple quantum circuits to represent $e^{\pm tR_i}$ operators. This analysis can be extended to higher-order PGCM^(k) formulations to include higher-rank excitations. It should be stressed that t_i parameters in Eqs. (23)–(30) can be chosen at random. The effects of random t_i parameters on ground-state FCI energies are illustrated in Appendix B.

V. GENERAL OUTLINE OF QUANTUM ALGORITHM AND POSTPROCESSING ON CONVENTIONAL COMPUTERS

After selecting GCM sampling points, the remaining work involves computing matrices ${\bf H}$ and ${\bf S}$ through Eqs. (13) and (14) using quantum computers. To accommodate gate-based quantum computers, the expectations are computed in the form

$$\mathbf{H}_{pq} = \sum_{j} h_{j} \langle \Phi | \left(e^{-\Gamma(\mathbf{Z}_{p})} P_{j} e^{\Gamma(\mathbf{Z}_{q})} \right) | \Phi \rangle$$
 (32)

and
$$\mathbf{S}_{pq} = \langle \Phi | \left(e^{-\Gamma(\mathbf{Z}_p)} e^{\Gamma(\mathbf{Z}_q)} \right) | \Phi \rangle,$$
 (33)

where Hamiltonian matrix H is transformed to the linear combination of Pauli strings $H = \sum_j h_j P_j$ under Jordan-Wigner (JW) transformation and $|\Phi\rangle$ is the HF state. The expectations can be easily evaluated using algorithms like the Hadamard test on fault-tolerant quantum computers. A pure quantum algorithm proposed for GCM and its complexity analysis is given in Appendix C, where we propose to exploit a block encoding for the operation \mathbf{S}^{-1} and use the phase estimation to compute the eigenvalues for the nonorthogonal eigenproblem (12). Note that the pure quantum algorithm gives a favorable scaling but relies on the use of the controlled unitary circuits

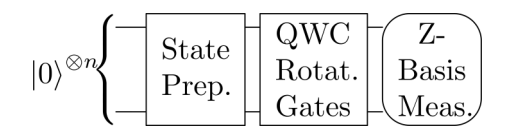


FIG. 3. Shallow circuit for Algorithm 1. The circuit is composed entirely of O(n) number of one-qubit gates, including state-preparation gates that initialize the ground state to the HF state and rotation gates for QWC, which employ one-qubit rotation gates to measure each wire in the Pauli-X, Y, or Z basis while the actual measurement is performed in the Pauli-Z basis.

that makes the quantum simulations on NISQ devices challenging.

For near-term devices, we focus on the hybrid quantumclassical approach where there is a trade-off between the depth of the quantum circuit and classical computation time. Note that, following the JW transformation, each of the operators R_1 to R_4 in Eqs. (24)–(27) can be transformed to four commuting Pauli strings. That is to say, the matrix exponential $e^{\pm t_i R_i}$ for $i \in \{1, 2, 3, 4\}$ are exactly the linear combinations of Pauli strings. So, for both H4 models, the calculations of expectation in Eqs. (32) and (33) are essentially equivalent to $\langle \Phi | P | \Phi \rangle$ for some Pauli string P, while qubitwise commuting (QWC) terms are grouped to perform a simultaneous measurement. The only implemented form of the circuit is illustrated in Fig. 3, and the whole process is summarized in Algorithm 1. The entire simulated quantum computation is achieved using Qiskit [61]. We put a brief discussion about trotterization under Qiskit in Appendix D, along with other implementation details related to duplicated Pauli strings and effects of random parameters in Appendix B.

VI. COMPLEXITY ANALYSIS AND EFFECTS OF FINITE **SAMPLINGS**

Recall that M is the number of selected **Z** points, which is equivalent to the number of sampling vectors. Let n be the number of spin-orbitals. We know the Hamiltonian matrix, H, consists of at most $O(n^4)$ Pauli strings, so operations for multiplying matrices and solving the generalized eigenvalue problem in Algorithm 1 dominate the classical part of the operation complexity. If an exponent of a cluster operator has up to c number of Pauli strings after trotterization and the multiplication between two length-n Pauli strings takes at most O(n) operations, then the matrix multiplication in lines 9 and 10 of Algorithm 1 takes $O(nc^2n^4)$ and $O(nc^2)$ operations, respectively, because all matrices are decomposed into the linear combinations of Pauli terms. As we have M^2 iterations in Algorithm 1 and the final generalized eigenvalue problem of $M \times M$ matrices takes $O(M^3)$ operations, QuGCM has the overall classical part of the worst-case scaling of $O(c^2n^5M^2 +$ M^3) operations.

The specific value of c highly depends on how users want to approximate the molecular models. It is affected by the number of creation and annihilation operators pairs in each single-excitation cluster operators, the value of k, and number of trotterization steps if it is necessary. As we discussed earlier, we can properly choose two pairs of creation and annihilation operators in each of single-excitation cluster op-

Algorithm 1. Quantum GCM (QuGCM) for near-term devices

Require: Hamiltonian matrix $H = \sum_{j} h_{j} P_{j}$, HF state $|\Phi\rangle$, and a set $\{\Gamma(\mathbf{Z}_i)\}_{i=1}^M$ where the index i could be a composite up to k terms as in Eq. (22)

- 1: Transform all $\{\Gamma(\mathbf{Z}_i)\}_{i=1}^M$ using JW transformation
- 2: Generate unitaries $\{V_i\}_{i=1}^M$ for $V_i := e^{\Gamma(\mathbf{Z}_i)}$ with Eq. (8) and
- 3: Trotterize each element in $\{V_i\}_{i=1}^M$ to a linear combination of Pauli strings
- 4: **for** each V_q in $\{V_i\}_{i=1}^M$ **do**
- 5: Compute $\sum_{i} h_{i} P_{j} V_{q}$ classically
- **for** each V_p in $\{V_i\}_{i=1}^M$ **do**
- Compute $\sum_{i} h_{j} V_{p}^{\dagger} (P_{j} V_{q})$ classically 7:
- 8:
- Compute $V_p^\dagger V_q$ classically Evaluate $\mathbf{H}_{pq}:=\sum_j h_j \langle \Phi|V_p^\dagger P_j V_q|\Phi \rangle$ in a quantum 9: device
- Evaluate $\mathbf{S}_{pq} := \langle \Phi | V_p^{\dagger} V_q | \Phi \rangle$ in a quantum device 10:
- 11: **end for**
- 12: **end for**
- 13: Solve the general eigenvalue problem $\mathbf{Hf} = E\mathbf{Sf}$ classically
- 14: return interested eigenvalues and eigenvectors

erators without the requirements of trotterization. The results in Sec. VII are promising enough when only single and double excitations are considered, i.e., when k = 2.

Regarding the quantum part of the operation complexity, it includes the number of circuits and the number of measurements in every circuit. Naively, line 9 and line 10 in Algorithm 1 indicate there are $O(M^2c^2n^4)$ number of and every circuit contains only O(n) number of one-qubit gates. Many existing methods can be applied to reduce the number of terms associated with $V_p^{\dagger}(HV_q)$ and $V_p^{\dagger}V_q$. For example, to reduce the order $O(M^2c^2n^4)$ to $O(M^2c^2n^{2\sim3})$ for the number of circuits in every iteration, the linear combination of unitaries technique [62], amplitude amplification approach [63], Hamiltonian simulation [64], qubitization [65], or the direct block-encoding [66] methods can be typically employed at the cost of introducing deeper circuits and implementing controlled unitary operations. Nevertheless, these approaches come with a probability of failure and require advanced circuit and error mitigation that might go beyond the capability of the current NISQ devices. Toward a more feasible NISQ approach, in light of the unitary partitioning scheme proposed by Izmaylov et al. [67], Peng and Kowalski recently proposed a more efficient unitary partitioning approach guided by the single-reference trial state used in the simulation [68]. In particular, through numerical tests over a wide range of molecules in different bases, we found that the nonunitary wave operators when acting on single-reference trial wave function (such as $e^{\Gamma(\mathbf{Z}_i)}|\Phi\rangle$ and $He^{\Gamma(\mathbf{Z}_i)}|\Phi\rangle$ in the present discussion) can be represented by a much more compact unitary basis, thus providing a more efficient route for performing the general nonunitary quantum simulations.

It is worth mentioning that the above discussion is focused on the number of terms/operations that can be efficiently reduced through groupings that feature the commutativity or anticommutativity of Pauli strings, while the total number of measurements required from the number of groups also critically depends on the covariance between the contributing terms, $cov(P_i, P_j)$, and the desired precision ϵ . Given that we can always write a matrix operator as a linear combination of Pauli strings, the total number of measurements for evaluating the expectation value of an operator with respect to the trial wave function can then be expressed as [69-71]

No. of Measurements

$$= \left(\frac{\sum_{G} \sqrt{\sum_{i,j,\in G} h_i h_j \text{cov}(P_i, P_j)}}{\epsilon}\right)^2$$
 (34)

with G indexing the groups. Therefore, it is likely that the number of groups decreases at the cost of introducing larger covariances that could essentially increase the total number of measurements required to achieve a desired precision. The variance of an individual Pauli string P_i can be bounded by

$$var(P_i) = \langle P_i^2 \rangle - \langle P_i \rangle^2 = 1 - \langle P_i \rangle^2 \leqslant 1, \tag{35}$$

which provides bounds to the covariance of any contributing terms

$$|\operatorname{cov}(P_i, P_j)| \leq \operatorname{var}(P_i)\operatorname{var}(P_j) \leq 1.$$
 (36)

Thus, according to Eq. (34), the bounds for the standard deviations of the matrix entry \mathbf{H}_{pq} and \mathbf{S}_{pq} under a finite number of measurements are

$$\epsilon_{\mathbf{H}_{pq}} \leqslant \frac{\sum_{G_{\mathbf{H}_{pq}}} \sqrt{\sum_{i,j,\epsilon G_{\mathbf{H}_{pq}}} |h_i h_j|}}{\sqrt{\text{No. of Measurements}}},$$
(37)

$$\epsilon_{\mathbf{S}_{pq}} \leqslant \frac{\sum_{G_{\mathbf{S}_{pq}}} \sqrt{\sum_{i,j,\epsilon G_{\mathbf{S}_{pq}}} |h_i h_j|}}{\sqrt{\text{No. of Measurements}}}.$$
 (38)

Let $\tilde{\mathbf{H}}_{pq}$ and $\tilde{\mathbf{S}}_{pq}$ be the entries computed from a finite number of measurements. We can empirically estimate the effects of the uncertainty by considering $\tilde{\mathbf{H}}_{pq}$ and $\tilde{\mathbf{S}}_{pq}$ as normal random variables

$$\tilde{\mathbf{H}}_{pq} \sim N(\mathbf{H}_{pq}, \epsilon_{\mathbf{H}_{pq}}^2) \text{ and } \tilde{\mathbf{S}}_{pq} \sim N(\mathbf{S}_{pq}, \epsilon_{\mathbf{S}_{pq}}^2).$$
 (39)

To illustrate the maximum possible fluctuations brought by finite-sampling errors, we set each $\epsilon_{\mathbf{H}_{pq}}$ and $\epsilon_{\mathbf{S}_{pq}}$ to their maximum as in Eq. (37) and Eq. (38), and summarize the results in Fig. 4. It is clear that to generally reach chemical accuracy, the $\alpha=0.005$ case requires about two orders of magnitude more measurements than the $\alpha=0.500$ case using Algorithm 1.

We also notice that there are also many other advanced measurement schemes proposed recently. One example is to simultaneously obtain expectation values of multiple observations by randomly measuring and projecting the quantum state into classical shadows [72–81]. In principle, the algorithm enables measurements of m low-weight observations using only $O(\log_2 m)$ samples. The practical performance of the algorithm for model and molecular Hamiltonians on NISQ devices, in terms of accuracy and efficiency, is still under intense study.

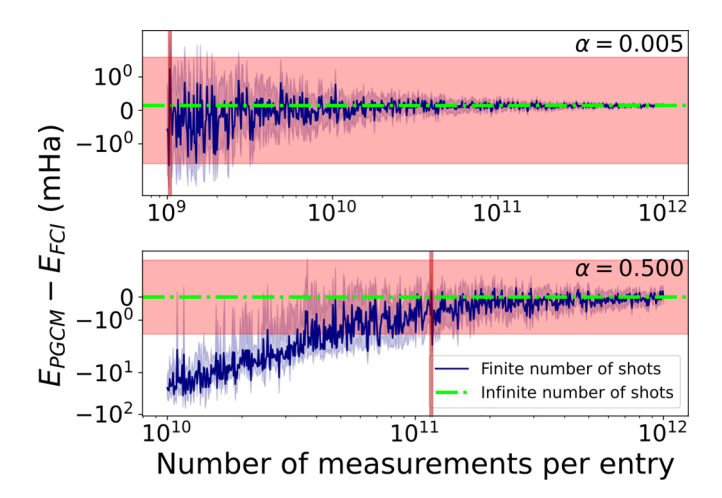


FIG. 4. Differences between the ground-state energy estimations from PGCM⁽²⁾ and FCI formalism in millihartrees for $\alpha=0.005$ (up) and $\alpha=0.500$ (down) H4 models, respectively. The variance of each random sampling is set to the maximum according to Eq. (37) and Eq. (38). The red-shaded region is the range of chemical accuracy ± 1.5936 mHa. The blue-shaded region is the 95% confidence interval estimated from 100 simulations with the red bars marking the rough number of measurement per entry at which the energy difference would be within the chemical accuracy.

VII. RESULTS

The GCM results for the ground-state energies and excitation energies corresponding to low-lying states of the symmetry of the reference function (singlet A_1 states) are collated in Tables I and II, respectively. To evaluate the accuracy of ground-state simulations, we compared GCM results with the results obtained with the RHF, multiconfigurational self-consistent field (MCSCF) [82] formalism for active space defined by four electrons and three active orbitals [MCSCF(4e, 3o)], configuration interaction method with singles and doubles (CISD), [83] CC method with singles and doubles (CCSD), [84,85] VQE formalism, and FCI formalism. We used the equation-of-motion CC approach (EOMCCSD) [86,87] and FCI formalism for excited states. Note that any quantum computation in VQE and GCM assumes infinite number of measurements.

Inspection of the results in Table I indicates that for both geometries, the GCM results are in very good agreement with the FCI result despite the simplicity of the expansions given by Eqs. (23)–(30). Interestingly, the GCM energies are significantly better in both cases than the VQE ones. The excellent performance of the GCM formalism is well illustrated by the

TABLE I. Differences (in millihartrees) with total ground-state FCI energies.

FCI	RHF	MCSCF(4e, 3o)	CISD	CCSD	VQE	GCM
H4 $\alpha = 0.005$						
-1.942993	151.407	82.645	5.507	3.331	0.905	0.147
H4 $\alpha = 0.500$						
-2.151007	75.764	43.276	1.866	0.003	0.058	0.022

TADIDI	O 1 .	• •			T 7
TABLE II.	Singlet	excitation	energies	1n	eV
mber ii.	Dingict	CACITUTION	Chichard	111	C .

Method	ω_1	ω_2	ω_3
	$H4 \alpha = 0$	0.005	
FCI	4.183	6.040	18.484
EOMCCSD	ICCSD 4.275		18.350
GCM	4.179	79 6.038	
	$H4 \alpha = 0$.500	
FCI	12.565	14.214	21.293
EOMCCSD	SD 12.738 14		21.255
GCM	12.589	14.840	21.622

strongly correlated $\alpha=0.005$ case, where CISD and CCSD methods struggle to capture needed correlation effects. For the weakly correlated variant of H4 ($\alpha=0.500$), the GCM formalism reproduces nearly FCI-level accuracy with an energy error of 0.022 millihartree.

In Table II we juxtaposed the excitation energies (ω_1 , ω_2 , and ω_3) obtained with the GCM approaches for three lowest-lying 1A_1 symmetry states, of H4 model for $\alpha=0.005$ and $\alpha=0.500$. For the ω_1 excitation energies, the GCM approach provides consistently better estimates of their exact (FCI) values than the ubiquitous EOMCCSD approach. While for ω_2 GCM prediction is better than the EOMCCSD one only for the $\alpha=0.005$, for the nondegenerate case ($\alpha=0.500$), the GCM prediction is by 0.6 eV off the FCI value. For the ω_3 excitation energies, the GCM is capable of providing estimates within 0.160 eV ($\alpha=0.005$) and 0.33 eV ($\alpha=0.500$) of error. Again, given the simplicity of the GCM formulations, one should view the GCM estimates of the excitation energies as quite satisfactory.

VIII. CONCLUSION

In this work we explored the use of the GCM in the context of quantum computing. For this purpose, we introduced the multiproduct extension of the GCM formalism that enables one to construct state vectors in Hilbert space using various types of the fermion Lie algebra and general quantum algorithms that allow one to perform GCM calculations in a way that can be viewed as a specific case of the quantum algorithms for configuration interaction formalisms involving a nonorthogonal basis. In the present study, we focused entirely on the U(N) algebra, where resulting state vectors can be interpreted in terms of the Thouless theorem. This analogy is essential in the sampling process of the parametrized unitary canonical transformations. It enables one to construct corresponding state vectors and corresponding linear space where higher-order excitations (e.g., double, triple, quadruple, etc.) can be selectively approached using the language of single excitations to define generators $[\Gamma(\mathbf{Z})]$ of the canonical transformations. The discussed procedures can be easily related to the searches of various type instabilities in independent particle formulations with the HF method as a specific example.

Using the H4 system as a benchmark, we showed that the quantum GCM algorithm could provide ground-state energies competitive to the VQE simulations involving the explicit form of the double excitations. In contrast to standard VQE

algorithms, the GCM formalism also yields the values of excited-state energies. We showed that GCM excitation energies corresponding to the low-lying excited states could be competitive with the excitation energies obtained with the popular EOMCCSD approach.

Although in the present form, the GCM formalism falls into the category of hybrid formulations, unlike the VQE method, it avoids multiple quantum-classical machine data transfer and unstable and tedious iterative processes. Also, our near-term implementation of the quantum GCM algorithm can run in parallel easily using multiple quantum and classical nodes.

Extension of the GCM-inspired quantum algorithms to larger systems in their ground and excited states will require the integrations of the recent advances in the development of compact representations of the wave function provided symmetry-projected Hartree-Fock (PHF) formulations [88–94] used to strongly correlated systems. The GCM and PHF-based methods are also well poised to be paired with different types of active-space downfolded Hamiltonians [95–97] that integrate the out-of-active-space (dynamical) correlation effects. In future studies, we plan to use the full potential of the quantum algorithms based on the quantum CI formulations and explore the possibility of using other types of fermionic algebras, i.e., SO(2N) and SO(2N+1)Lie algebras in the context of quantum simulations of strongly correlated systems defined by Hubbard, Bose-Hubbard, Ising, and various impurity models.

The code and data in the paper are openly available in the GitHub repository [98].

ACKNOWLEDGMENTS

M.Z., B.P., N.W., A.L., and K.K. were supported by the "Embedding QC into Many-Body Frameworks for Strongly Correlated Molecular and Materials Systems" project, which is funded by the U.S. Department of Energy, Office of Science, Office of Basic Energy Sciences, Division of Chemical Sciences, Geosciences, and Biosciences. The Pacific Northwest National Laboratory is operated by Battelle for the U.S. Department of Energy under Contract No. DE-AC05-76RL01830. X.Y. was supported by National Science Foundation CAREER DMS-2143915. M.Z. and X.Y. both also were supported by the Defense Advanced Research Projects Agency (DARPA) as part of Project No. W911NF2010022, "The Quantum Computing Revolution and Optimization: Challenges and Opportunities."

APPENDIX A: THOULESS THEOREM AND INSTABILITIES OF HARTREE-FOCK SOLUTIONS

The use of the Thouless theorem in search of the instabilities of HF solutions has been broadly discussed in the literature (see, e.g., Refs. [44,58–60,99–101]). Here we discuss only the basic tenets of this approach.

The original form of the Thouless theorem states that two nonorthogonal determinants $|\Phi\rangle$ (corresponding to some HF solution) and $|\Phi'\rangle$ in its vicinity can be interrelated by the

exponential ansatz

$$|\Phi'\rangle = e^{T_1}|\Phi\rangle,\tag{A1}$$

where the T_1 operator is defined as

$$T_1 = \sum_{i,a} t_i^a a_a^{\dagger} a_i, \tag{A2}$$

where indices i (a) refer to spin orbitals occupied (unoccupied) in $|\Phi\rangle$. Therefore the local behavior of the energy functional in the neighborhood of the HF solution can be parametrized as a function of scalar amplitudes t_i^a :

$$E(\lbrace t_i^a \rbrace) = \frac{\langle \Phi'(\lbrace t_i^a \rbrace) | H | \Phi'(\lbrace t_i^a \rbrace) \rangle}{\langle \Phi'(\lbrace t_i^a \rbrace) | \Phi'(\lbrace t_i^a \rbrace) \rangle}. \tag{A3}$$

Its second-order variation, $\delta^{(2)}E$, of (A3) (the first-order variation disappears as a consequence of the Brillouin condition) can be expressed as

$$\delta^{(2)}E = (\mathbf{T} \quad \bar{\mathbf{T}}) \begin{pmatrix} \mathbf{A} & \mathbf{B} \\ \bar{\mathbf{B}} & \bar{\mathbf{A}} \end{pmatrix} \begin{pmatrix} \mathbf{T} \\ \bar{\mathbf{T}} \end{pmatrix}$$
$$= \mathbf{D}^{\dagger} \mathbf{L} \mathbf{D}, \tag{A4}$$

where **T** is a vector of t_i^a amplitudes and $\bar{\mathbf{T}}$ is complex conjugate of **T**. The matrices **A** and **B** can be expressed as

$$A_{\{i,a\},\{j,b\}} = \langle a_a^{\dagger} a_i \Phi | H_N | a_b^{\dagger} a_j \Phi \rangle, \tag{A5}$$

$$B_{\{i,a\},\{j,b\}} = \langle a_a^{\dagger} a_i a_b^{\dagger} a_j \Phi | H_N | \Phi \rangle, \tag{A6}$$

where H_N designates the Hamiltonian operator in the normal product form, $H_N = H - \langle \Phi | H | \Phi \rangle$. For the HF solution to be stable, all eigenvalues of matrix **L** must be positive. Otherwise, there exists a Slater determinant in the vicinity of $|\Phi\rangle$ that provides lower energy than the HF energy corresponding to the Slater determinant $|\Phi\rangle$. If **A** and **B** matrices are real, then $\delta^{(2)}E$ can be rearranged in the form

$$\delta^{(2)}E = \frac{1}{4}[(\mathbf{T} + \bar{\mathbf{T}})^{\dagger}(\mathbf{A} + \mathbf{B})(\mathbf{T} + \bar{\mathbf{T}})$$
$$+ (\mathbf{T} - \bar{\mathbf{T}})^{\dagger}(\mathbf{A} - \mathbf{B})(\mathbf{T} - \bar{\mathbf{T}})], \tag{A7}$$

and the nature of real instabilities can be explored by analyzing eigenvalues of the $\mathbf{A} + \mathbf{B}$ matrix, whereas the purely complex (imaginary) instabilities are associated with the eigenvalues of the $\mathbf{A} - \mathbf{B}$ matrix.

The Thouless theorem gives a good insight into the mechanism of the instability generation. Let us assume that the exact wave function ($|\Psi\rangle$) expansion in intermediate normalization ($\langle\Psi|\Phi\rangle=1$) is dominated by the HF Slater determinant and Slater determinant $|\Phi_{i\bar{i}}^{a\bar{a}}\rangle$ obtained by promoting two α and β electrons from the same orbital (the corresponding spin orbitals are denoted as i and \bar{i}) to some virtual orbital (the corresponding spin orbitals are denoted as a and \bar{a}),

$$|\Psi\rangle = |\Phi\rangle + \dots + c_{i\bar{i}}^{a\bar{a}} |\Phi_{i\bar{i}}^{a\bar{a}}\rangle + \dots,$$
 (A8)

where coefficient $c_{ii}^{a\bar{a}}$ is negative (a typical situation encountered in a single bond breaking process). To recover this correlation effect by Thouless expansion (A1) one has

$$c_{i\bar{i}}^{a\bar{a}} \simeq t_i^a t_{\bar{i}}^{\bar{a}}.\tag{A9}$$

If additionally the T_1 operator is not breaking a spin symmetry, i.e., $t_i^a = t_{\bar{i}}^{\bar{a}}$ then from (A8) t_i^a and $t_{\bar{i}}^{\bar{a}}$ are purely imaginary.

TABLE III. Number of unique Pauli terms and their ratios after grouping among all iterations.

	No. of unique terms	Total no. of terms	Ratio (%)	
	H4 a	$\alpha = 0.005$		
\mathbf{S}	1444	38 904	3.71%	
H	3423	118 426	2.89%	
All	4180	157 330	2.66%	
	H4 a	$\alpha = 0.500$		
\mathbf{S}	1766	38 888	4.54%	
Н	3454	118 621	2.91%	
All	4370	157 509	2.77%	

The Thouless theorem also provides the understanding of mechanisms behind other types of instabilities.

APPENDIX B: DUPLICATED PAULI STRINGS AND SELECTION OF PARAMETERS

For each of H4 models, while M = 15, the symmetries of **H** and **S** allow us to compute only 120 iterations instead of 225 iterations. Among those 120 iterations, as shown in Table III, we only need to measure around 4000 Pauli strings because more than 97% of them are duplicated. This brings the two orders of magnitude reduction on the total number of measurements in practice.

Meanwhile, we conducted the following experiments for $\alpha = 0.005$ and $\alpha = 0.500$ H4 models to demonstrate the influence of the random choices of t_i parameters on the estimations of the ground-state FCI energies. For each molecular model, we generated 50 sets of $\{t_i\}_{i=1}^7$ for t_i in [0,1), [0,100), and [100,100), respectively. Each of 300 sets of $\{t_i\}_{i=1}^7$ produced an estimation of the ground-state FCI energy from Algorithm 1 (assume an infinite number of shots). The distributions of differences between the estimations from PGCM⁽²⁾ and FCI formalism under various settings are illustrated in Fig. 5 using box plots. It worth noting that when we produce t_i from [0,1), about 25% random generations can provide an estimation of ground-state energy within the range of chemical accuracy.

APPENDIX C: LINEAR-SYSTEM-INSPIRED ALGORITHMS FOR GCM

Perhaps the most direct way to use quantum computing to solve the electronic structure problem using Generator Coordinate Methods is by simply solving the nonorthogonal eigenvalue problem by dilating it to a square matrix in a higher dimensional space. In this case, it is most convenient to express our eigenvalue problem as

$$\mathbf{S}^{-1}\mathbf{H}\mathbf{f} = E\mathbf{f},\tag{C1}$$

where we have assumed here that S is an invertible matrix. Now let us define an isometric extension of our original space. We do this to exploit a block encoding for the operation S^{-1} , which allows us to express it as a unitary operation in a higher dimensional space. Specifically, let

$$\mathbf{U} = \begin{bmatrix} \mathbf{S}^{-1} / \| \mathbf{S}^{-1} \| & \square \\ \square & \square \end{bmatrix}$$
 (C2)

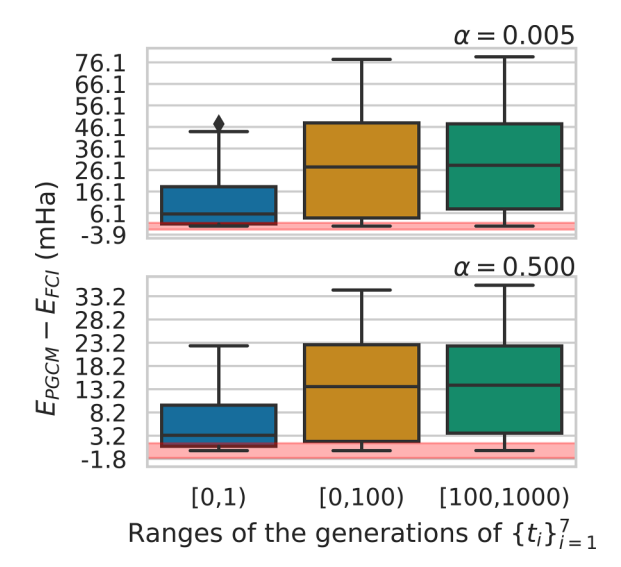


FIG. 5. Differences between the ground-state energy estimations from PGCM⁽²⁾ in various random $\{t_i\}$'s and FCI formalism in millihartrees for $\alpha=0.005$ (up) and $\alpha=0.500$ (down) H4 models, respectively. The horizontal red-shaded region shows the range of chemical accuracy ± 1.5936 mHa. That minimum value and the 25th percentile are in the shaded region when $t_i \in [0,1)$ in both H4 models indicates that random generations of t_i in that range are relatively likely to provide a good approximation in our algorithm.

be a unitary matrix (i.e., $\mathbf{U}^{\dagger} = \mathbf{U}^{-1}$) for arbitrary matrices \square . Also let

$$\mathbf{J} = \begin{bmatrix} \mathbf{H}/\alpha & 0 \\ 0 & 0 \end{bmatrix}, \ \mathbf{g} = \begin{bmatrix} \mathbf{f} \\ 0 \end{bmatrix}, \ \mathbf{Z} = \begin{bmatrix} \mathbf{I} & 0 \\ 0 & -\mathbf{I} \end{bmatrix}, \ \mathbf{P} = \frac{1}{2}(\mathbf{I} + \mathbf{Z}).$$
(C3)

Inside this enlarged space, the eigenvalue equation reads for eigenvalue E

$$\mathbf{PUJPg} = \frac{E\mathbf{g}}{\|\mathbf{S}^{-1}\|\alpha}.$$
 (C4)

Now let $\mathbf{H}/\alpha = \sum_{j} h_{j} \mathbf{U}_{j}^{(H)}$ for a set of unitary $\mathbf{U}_{j}^{(H)}$. We then have that our Hamiltonian in the enlarged space can be expressed as a similar linear combination of unitaries.

$$\mathbf{J} = \sum_{j} h_{j} |0\rangle\langle 0| \otimes \mathbf{U}_{j}^{(H)} = \sum_{j} \frac{h_{j}}{2} (\mathbf{I} \otimes \mathbf{U}_{j}^{(H)} + \mathbf{Z} \otimes \mathbf{U}_{j}^{(H)}).$$
(C5)

Thus the entire product can be expressed as

$$\mathbf{PUJP} = \sum_{j} \frac{h_{j}}{2} \mathbf{P} \left[\mathbf{U} \left(\mathbf{I} \otimes \mathbf{U}_{j}^{(H)} \right) + \mathbf{U} \left(\mathbf{Z} \otimes \mathbf{U}_{j}^{(H)} \right) \right] \mathbf{P}. \quad (C6)$$

Thus the enlarged Hamiltonian **J** can be expressed as a linear combination of unitary matrices that further has the exact same value of $\alpha = \sum_{i} |h_{i}|$.

For us to use phase estimation to compute these eigenvalues, we also need a further modification. Note that e^{-iUJ} is not necessarily unitary because UJ is not necessarily Hermitian. We address this issue by considering a further embedding:

$$\mathbf{K} = \begin{bmatrix} 0 & \mathbf{PUJP} \\ \mathbf{PJU}^{\dagger}\mathbf{P} & 0 \end{bmatrix}$$
$$= |0\rangle\langle 1| \otimes \mathbf{PUJP} + |1\rangle\langle 0| \otimes \mathbf{PJU}^{\dagger}\mathbf{P}$$

$$= \frac{1}{2} (\mathbf{X} \otimes \mathbf{PUJP} + (i\mathbf{Y}) \otimes \mathbf{PUJP} + \mathbf{X} \otimes \mathbf{PJU}^{\dagger} \mathbf{P} + (-i\mathbf{Y}) \otimes \mathbf{PJU}^{\dagger} \mathbf{P}).$$
(C7)

This expression also takes the form of a linear combination of unitary matrices; however, the coefficient sum now obeys $\sum_j |h_j'| = 2\alpha$, which does not change the overall complexity. Finally note that **K** is antidiagonal block matrix. We can therefore search for an eigenvector of the form $\mathbf{h} = [0 \ \mathbf{g}]^{\dagger}$ as the eigenvectors of **K** can be taken to have support only on one of the two blocks. The eigenvalues of **K** corresponding the the eigenvector \mathbf{g} of **PUJP** must be $\pm E$ from this construction. To see this note that

$$\operatorname{Tr}(\mathbf{K}^2\mathbf{h}\mathbf{h}^{\dagger}) = \operatorname{Tr}(\mathbf{h}^{\dagger}\mathbf{K}^2\mathbf{h}) = (\mathbf{K}\mathbf{h})^{\dagger}(\mathbf{K}\mathbf{h}) = E^2.$$
 (C8)

Thus **h** is an eigenvector of **K** and the eigenvalues of **K** in the support of **h** must be $\pm E$. Thus, we can estimate the absolute value of E by using phase estimation on **K**.

To perform this simulation using qubitization ideas, we will need to propose *prepare-and-select* circuits for the coefficients. Specifically,

$$U_{\text{prep}} |0\rangle = \sum_{i} \sum_{\mu=0.1} \sum_{\nu=0.1} \sum_{\omega=0.1} \frac{\sqrt{h_j/4}}{\sqrt{2\alpha}} |j\rangle |\mu\rangle |\nu\rangle |\omega\rangle \quad (C9)$$

and further

$$U_{\text{sel}} |j\rangle |\mu\rangle |\nu\rangle |\omega\rangle |\psi\rangle = |j\rangle |\mu\rangle |\nu\rangle |\omega\rangle$$

$$\otimes (-1)^{\mu\omega} \mathbf{X}^{\mu} (i\mathbf{Y})^{1-\mu} \otimes \mathbf{Z}^{\nu}$$

$$\otimes \mathbf{U}^{\dagger\omega} \mathbf{U}_{i}^{(H)} \mathbf{U}^{1-\omega} |\psi\rangle . \qquad (C10)$$

This then forms a block encoding of our operator for the generalized eigenvalue problem:

$$(\langle 0| \otimes \mathbf{I})U_{\text{prep}}^{\dagger}U_{\text{sel}}U_{\text{prep}}(|0\rangle \otimes \mathbf{I}) = \mathbf{K}/(2\alpha). \tag{C11}$$

Using qubitization, we can convert this into a unitary with result [66], and we can perform phase estimation to learn E with a variance of at most ϵ^2 using a number of queries to U_{sel} and U_{prep} that is in $O(\alpha \| \mathbf{S}^{-1} \| / \epsilon)$. However, each application of U_{sel} requires O(1) queries to \mathbf{U} , which is a block encoding of the inverse of \mathbf{S} . A deeper analysis of the cost is possible; however, to do this, we first need to have consensus on the input model used for the simulation.

The easiest way to compute a matrix element for the overlap matrix is through the use of a controlled unitary. The overlap of the estimate takes the form

$$\langle \Phi | V_p^{\dagger} V_q | \Phi \rangle = \mathbf{S}_{p,q},$$
 (C12)

where V_p is the basis transform operation such that for the reference state $|\Phi\rangle$, $V_p |\Phi\rangle = |\Phi(\mathbf{Z}_p)\rangle$. To use the Hadamard test to reconstruct this circuit we require a single application of V_p^{\dagger} and a single application of V_q . The probability that the control qubit that governs this circuit is 0 is

$$P(0|p,q) = \frac{1 + \text{Re}(\langle \Phi(\mathbf{Z}_p) | \Phi(\mathbf{Z}_q) \rangle)}{2}.$$
 (C13)

If needed, the imaginary part can be similarly found by applying an S^{\dagger} gate to the control. If we apply amplitude amplification to the result, then we can construct a matrix

AA(P) with eigenvalues inside the sector:

$$\lambda(\mathbf{A}\mathbf{A}(\mathbf{P})) = e^{\pm i\cos^{-1}\left(\sqrt{\frac{1+\operatorname{Re}(\langle\Phi(Z_p)|\Phi(Z_q)\rangle)}{2}}\right)}$$
(C14)

and is equivalent to the following matrix in the twodimensional space spanned by the initial state and the marked state:

$$\begin{bmatrix}
\sqrt{\frac{1+\operatorname{Re}(\langle \Phi(Z_p)|\Phi(Z_q)\rangle)}{2}} & -\sqrt{\frac{1-\operatorname{Re}(\langle \Phi(Z_p)|\Phi(Z_q)\rangle)}{2}} \\
\sqrt{\frac{1-\operatorname{Re}(\langle \Phi(Z_p)|\Phi(Z_q)\rangle)}{2}} & \sqrt{\frac{1+\operatorname{Re}(\langle \Phi(Z_p)|\Phi(Z_q)\rangle)}{2}}
\end{bmatrix}.$$
(C15)

Applying quantum signal processing we can apply a transformation $u \mapsto 2u^2 - 1$. Note that this is (1) an even degree polynomial and (2) it is between [-1, 1] for u in a similar range. This means that quantum signal processing can be used to apply this transformation on the top block of the matrix to prepare a block encoding of the form [66]

$$U_{\mathbf{S}} = \begin{bmatrix} \mathbf{Re}(\langle \Phi(Z_p) | \Phi(Z_q) \rangle) & \Box \\ \Box & \Box \end{bmatrix}, \quad (C16)$$

where specifically we have that the initial state used in the amplitude amplification routine block-encodes the overlap matrix **S**. In all, this process costs $O(\text{polylog}(1/\epsilon))$ queries to the state preparation oracle to produce this block encoding.

Next we need to prepare a block encoding of S^{-1} . Using the results of Ref. [102] we can prepare such a block encoding using $O(\|\mathbf{S}\|\|\mathbf{S}^{-1}\|\text{polylog}(1/\epsilon))$ queries where ϵ is our target accuracy. Thus, the overall query complexity is the number of queries made to \mathbf{K} multiplied by the number of queries per U or $U_j^{(H)}$. The former result then shows that the final cost of the simulation using this approach (in terms of queries to the prepare-and-select oracles of \mathbf{H} and the queries to Z_p, Z_q) scales as

$$\tilde{O}\left(\frac{\alpha \|\mathbf{S}\| \|\mathbf{S}^{-1}\|^2}{\epsilon}\right). \tag{C17}$$

This shows that the query complexity of the simulation using this approach does not necessarily scale with the dimension of the space. It does, however, depend strongly on the one-norm of the coefficients of the Hamiltonian and the norm of the inverse of the overlap matrix. Thus, the worse conditioned the matrix is, the worse we expect the performance of the algorithm to be. In contrast, learning the matrix S in high-dimensional spaces to perform the inverse can be expensive as noted in the main text. This approach gives a theoretical alternative in such cases that has favorable scaling asymptotically at the price of the algorithm requiring a large number of qubits.

APPENDIX D: TROTTERIZATION OF A MATRIX EXPONENTIAL

This section aims to transform a matrix exponential into a linear combination of Pauli group matrices. Because the standard form of a matrix exponential in Qiskit is e^{-itA} instead of e^{tA} as we have in the main body for some parameter t and matrix A and we implemented the quantum part of our algorithm in Qiskit, we keep $i = \sqrt{-1}$ in the power. Because we will use a dot product between matrices, we do not omit the operator \otimes when we do the Kronecker product between

Pauli matrices for clarity (e.g., XY means the dot product of X and Y instead of $X \otimes Y$). Let n be the number of qubits, I_n the identity matrix in space $\mathbb{C}^{2^n} \times \mathbb{C}^{2^n}$, and $P \in \{X, Y, Z, I\}^{\otimes n}$ an n-qubit Pauli group matrix. Then, for any n-qubit Pauli group matrix, we have

$$P^{2} = \left(\bigotimes_{l=1}^{n} \sigma_{l}\right) \left(\bigotimes_{l=1}^{n} \sigma_{l}\right) = \left(\bigotimes_{l=1}^{n} \sigma_{l}^{2}\right) = I_{n}$$
 (D1)

given $\sigma_l^2 = I$, for all $\sigma_l \in \{X, Y, Z, I\}$ and the property of Kronecker product

$$(A \otimes B)(C \otimes D) = (AC) \otimes (BD) \tag{D2}$$

for some matrices A, B, C, D in the appropriate dimensions.

Now, by doing Taylor expansion of e^{itP} at t = 0, we obtain the following exact conversion:

$$e^{itP} = I_n + (itP) + \frac{(itP)^2}{2!} + \frac{(itP)^3}{3!} + \frac{(itP)^4}{4!} + \frac{(itP)^5}{5!} \cdots$$

$$= I_n + itP - I_n \frac{t^2}{2} - iP \frac{t^3}{3!} + I_n \frac{t^4}{4} + iP \frac{t^5}{5!} \cdots$$

$$= I_n \left(1 - \frac{t^2}{2} + \frac{t^4}{4} + \cdots \right) + iP \left(t - \frac{t^3}{3!} + \frac{t^5}{5!} + \cdots \right)$$

$$= \cos(t)I_n + i\sin(t)P, \tag{D3}$$

where t is a scalar parameter. If we deal with more than a single Pauli group matrix, then we need to use Suzuki trotterization. For $P_l \in \{X, Y, Z, I\}^{\otimes n}$, the first-order Suzuki trotterization is

$$e^{-i\sum_{l=1}^{m} s_l P_l} = \prod_{l=1}^{m} e^{-is_l P_l} + O(m^2 s^2),$$
 (D4)

where $s := \max_{l} s_{l}$. So for large t, to control error, we need to separate the evolution into multiple steps:

$$e^{-i\sum_{l=1}^{m} s_l P_l} = \left(\prod_{k=1}^{m} e^{-i(s_l/r)P_l}\right)^r + O(m^2 s^2/r),$$
 (D5)

where r is the number of evolution steps. There is also a second-order formula for smaller error:

$$e^{-i\sum_{l=1}^{m} s_l P_l} = \left(\prod_{l=1}^{m} e^{-i\frac{s_l}{2r}P_l} \prod_{l=m}^{1} e^{-i\frac{s_l}{2r}P_l}\right)^r + O(m^3 s^3/r^2).$$
 (D6)

So, if we set the trotterization error level at ϵ , then we need to split the evolution into $r \in O(\frac{m^{3/2}s^{3/2}}{\sqrt{\epsilon}})$ steps with the

second-order formula. By choosing $t = -\frac{s}{2r}$, Eq. (D3) gives

$$e^{-i\frac{s}{2r}P} = \cos\left(\frac{s}{2r}\right)I_n - i\sin\left(\frac{s}{2r}\right)P. \tag{D7}$$

As a result, Eq. (D6) becomes

$$e^{-i\sum_{l=1}^{m} s_l P_l} \approx \left(\prod_{l=1}^{m} \left[\cos\left(\frac{s_l}{2r}\right) I_n - i \sin\left(\frac{s_l}{2r}\right) P_l \right] \prod_{l=m}^{1} \left[\cos\left(\frac{s_l}{2r}\right) I_n - i \sin\left(\frac{s_l}{2r}\right) P_l \right] \right)^r. \tag{D8}$$

In this case, we approximate the exponential of the linear combination of the Pauli group matrices by another linear combination of Pauli group matrices, where the expectation of the latter one can be evaluated in a gate-based quantum computer easily. Note that in the r=1 case, if we have m terms in the power, we end up with at most $O(m^2)$ terms after the transformation, which is exactly the scenario we had in H4 examples in the main text.

- [1] A. Luis and J. Peřina, Optimum phase-shift estimation and the quantum description of the phase difference, Phys. Rev. A **54**, 4564 (1996).
- [2] R. Cleve, A. Ekert, C. Macchiavello, and M. Mosca, Quantum algorithms revisited, Proc. R. Soc. London A 454, 339 (1998).
- [3] D. W. Berry, G. Ahokas, R. Cleve, and B. C. Sanders, Efficient quantum algorithms for simulating sparse Hamiltonians, Commun. Math. Phys. 270, 359 (2007).
- [4] A. M. Childs, On the relationship between continuous-and discrete-time quantum walk, Commun. Math. Phys. 294, 581 (2010).
- [5] D. Wecker, M. B. Hastings, and M. Troyer, Progress towards practical quantum variational algorithms, Phys. Rev. A 92, 042303 (2015).
- [6] T. Häner, D. S. Steiger, M. Smelyanskiy, and M. Troyer, High performance emulation of quantum circuits, in SC '16: Proceedings of the International Conference for High Performance Computing, Networking, Storage and Analysis (IEEE, Piscataway, NJ, 2016), p. 866.
- [7] D. Poulin, A. Kitaev, D. S. Steiger, M. B. Hastings, and M. Troyer, Fast Quantum Algorithm for Spectral Properties, Phys. Rev. Lett. 121, 010501 (2018).
- [8] A. Peruzzo, J. R. McClean, P. Shadbolt, M.-H. Yung, X.-Q. Zhou, P. J Love, A. Aspuru-Guzik, and J. L. O'Brien, A variational eigenvalue solver on a photonic quantum processor, Nat. Commun. 5, 4213 (2014).
- [9] J. R. McClean, J. Romero, R. Babbush, and A. Aspuru-Guzik, The theory of variational hybrid quantum-classical algorithms, New J. Phys. 18, 023023 (2016).
- [10] J. Romero, R. Babbush, J. R. McClean, C. Hempel, P. J. Love, and A. Aspuru-Guzik, Strategies for quantum computing molecular energies using the unitary coupled cluster ansatz, Quantum Sci. Technol. 4, 014008 (2018).
- [11] Y. Shen, X. Zhang, S. Zhang, J.-N. Zhang, M.-H. Yung, and K. Kim, Quantum implementation of the unitary coupled cluster for simulating molecular electronic structure, Phys. Rev. A 95, 020501(R) (2017).
- [12] A. Kandala, A. Mezzacapo, K. Temme, M. Takita, M. Brink, J. M. Chow, and J. M. Gambetta, Hardware-efficient variational quantum eigensolver for small molecules and quantum magnets, Nature (London) 549, 242 (2017).

- [13] A. Kandala, K. Temme, A. D. Córcoles, A. Mezzacapo, J. M. Chow, and J. M. Gambetta, Error mitigation extends the computational reach of a noisy quantum processor, Nature (London) 567, 491 (2019).
- [14] J. I. Colless, V. V. Ramasesh, D. Dahlen, M. S. Blok, M. E. Kimchi-Schwartz, J. R. McClean, J. Carter, W. A. de Jong, and I. Siddiqi, Computation of Molecular Spectra on a Quantum Processor with an Error-Resilient Algorithm, Phys. Rev. X 8, 011021 (2018).
- [15] W. J. Huggins, J. Lee, U. Baek, B. O'Gorman, and K. B. Whaley, A non-orthogonal variational quantum eigensolver, New J. Phys. 22, 073009 (2020).
- [16] I. G. Ryabinkin, T.-C. Yen, S. N. Genin, and A. F. Izmaylov, Qubit coupled cluster method: A systematic approach to quantum chemistry on a quantum computer, J. Chem. Theory Comput. 14, 6317 (2018).
- [17] Y. Cao, J. Romero, J. P. Olson, M. Degroote, P. D. Johnson, M. Kieferová, I. D. Kivlichan, T. Menke, B. Peropadre, N. P. D. Sawaya *et al.*, Quantum chemistry in the age of quantum computing, Chem. Rev. 119, 10856 (2019).
- [18] I. G. Ryabinkin, R. A. Lang, S. N. Genin, and A. F. Izmaylov, Iterative qubit coupled cluster approach with efficient screening of generators, J. Chem. Theory Comput. 16, 1055 (2020).
- [19] A. F. Izmaylov, T.-C. Yen, R. A. Lang, and V. Verteletskyi, Unitary partitioning approach to the measurement problem in the variational quantum eigensolver method, J. Chem. Theory Comput. 16, 190 (2020).
- [20] R. A. Lang, I. G. Ryabinkin, and A. F. Izmaylov, Unitary transformation of the electronic Hamiltonian with an exact quadratic truncation of the Baker-Campbell-Hausdorff expansion, J. Chem. Theory Comput. 17, 66 (2021).
- [21] H. R. Grimsley, S. E. Economou, E. Barnes, and N. J. Mayhall, An adaptive variational algorithm for exact molecular simulations on a quantum computer, Nat. Commun. 10, 3007 (2019).
- [22] H. R. Grimsley, D. Claudino, S. E. Economou, E. Barnes, and N. J. Mayhall, Is the trotterized UCCSD ansatz chemically well-defined? J. Chem. Theory Comput. 16, 1 (2020).
- [23] M. Cerezo, A. Arrasmith, R. Babbush, S. C. Benjamin, S. Endo, K. Fujii, J. R. McClean, K. Mitarai, X. Yuan, L. Cincio et al., Variational quantum algorithms, Nat. Rev. Phys. 3, 625 (2021).

- [24] S. McArdle, S. Endo, A. Aspuru-Guzik, S. C. Benjamin, and X. Yuan, Quantum computational chemistry, Rev. Mod. Phys. **92**, 015003 (2020).
- [25] K. Bharti, A. Cervera-Lierta, T. H. Kyaw, T. Haug, S. Alperin-Lea, A. Anand, M. Degroote, H. Heimonen, J. S. Kottmann, T. Menke *et al.*, Noisy intermediate-scale quantum algorithms, Rev. Mod. Phys. 94, 015004 (2022).
- [26] A. Anand, P. Schleich, S. Alperin-Lea, P. W. K. Jensen, S. Sim, M. Díaz-Tinoco, J. S. Kottmann, M. Degroote, A. F. Izmaylov, and A. Aspuru-Guzik, A quantum computing view on unitary coupled cluster theory, Chem. Soc. Rev. 51, 1659 (2022).
- [27] R. J. Bartlett, S. A. Kucharski, and J. Noga, Alternative coupled-cluster ansätze II. The unitary coupled-cluster method, Chem. Phys. Lett. **155**, 133 (1989).
- [28] A. G. Taube and R. J. Bartlett, New perspectives on unitary coupled-cluster theory, Int. J. Quantum Chem. 106, 3393 (2006)
- [29] M. R. Hoffmann and J. Simons, A unitary multiconfigurational coupled-cluster method: Theory and applications, J. Chem. Phys. 88, 993 (1988).
- [30] W. Kutzelnigg, Error analysis and improvements of coupledcluster theory, Theor. Chim. Acta 80, 349 (1991).
- [31] F. A. Evangelista, G. K.-L. Chan, and G. E. Scuseria, Exact parameterization of fermionic wave functions via unitary coupled cluster theory, J. Chem. Phys. 151, 244112 (2019).
- [32] K. Kowalski, Dimensionality reduction of the many-body problem using coupled-cluster subsystem flow equations: Classical and quantum computing perspective, Phys. Rev. A **104**, 032804 (2021).
- [33] D. L. Hill and J. A. Wheeler, Nuclear constitution and the interpretation of fission phenomena, Phys. Rev. 89, 1102 (1953).
- [34] R. Rodríguez-Guzmán, J. L. Egido, and L. M. Robledo, Correlations beyond the mean field in magnesium isotopes: Angular momentum projection and configuration mixing, Nucl. Phys. A 709, 201 (2002).
- [35] M. Bender, P.-H. Heenen, and P.-G. Reinhard, Self-consistent mean-field models for nuclear structure, Rev. Mod. Phys. **75**, 121 (2003).
- [36] P. Ring and P. Schuck, *The nuclear Many-Body Problem* (Springer Science & Business Media, Berlin, Heidelberg, New York, 2004).
- [37] J. M. Yao, J. Meng, P. Ring, and D. Vretenar, Configuration mixing of angular-momentum-projected triaxial relativistic mean-field wave functions, Phys. Rev. C 81, 044311 (2010).
- [38] J. L. Egido, State-of-the-art of beyond mean field theories with nuclear density functionals, Phys. Scr. **91**, 073003 (2016).
- [39] N. Hizawa, K. Hagino, and K. Yoshida, Generator coordinate method with a conjugate momentum: Application to particle number projection, Phys. Rev. C 103, 034313 (2021).
- [40] J. R. Klauder and B.-S. Skagerstam, Coherent States: Applications in Physics and Mathematical Physics (World Scientific, 1985)
- [41] W.-M. Zhang, D. H. Feng, and R. Gilmore, Coherent states: Theory and some applications, Rev. Mod. Phys. **62**, 867 (1990).
- [42] H. Fukutome, The group theoretical structure of fermion many-body systems arising from the canonical anticommutation relation. I: Lie algebras of fermion operators and exact

- generator coordinate representations of state vectors, Prog. Theor. Phys. **65**, 809 (1981).
- [43] K. Goeke and P.-G. Reinhard, The generator-coordinatemethod with conjugate parameters and the unification of microscopic theories for large amplitude collective motion, Ann. Phys. 124, 249 (1980).
- [44] H. Fukutome, Unrestricted Hartree–Fock theory and its applications to molecules and chemical reactions, Int. J. Quantum Chem. **20**, 955 (1981).
- [45] J. Paldus, Many-electron correlation problem. A group theoretical approach, in *Theoretical Chemistry* (Elsevier, 1976), Vol. 2, pp. 131–290.
- [46] J. Paldus and B. Jeziorski, Clifford algebra and unitary group formulations of the many-electron problem, Theor. Chim. Acta 73, 81 (1988).
- [47] R. Jozsa and A. Miyake, Matchgates and classical simulation of quantum circuits, Proc. R. Soc. A 464, 3089 (2008).
- [48] A. F. Izmaylov, M. Díaz-Tinoco, and R. A. Lang, On the order problem in construction of unitary operators for the variational quantum eigensolver, Phys. Chem. Chem. Phys. **22**, 12980 (2020).
- [49] T.-C. Yen and A. F. Izmaylov, Cartan subalgebra approach to efficient measurements of quantum observables, PRX Quantum 2, 040320 (2021).
- [50] K. Goeke and P.-G. Reinhard, A consistent microscopic theory of collective motion in the framework of an ATDHF approach, Ann. Phys. **112**, 328 (1978).
- [51] P.-G. Reinhard and K. Goeke, Reality conditions for classical motions along collective paths, Phys. Rev. C 17, 1249 (1978).
- [52] P.-G. Reinhard and K. Goeke, The concept of a collective path and its range of validity, Nucl. Phys. A 312, 121 (1978).
- [53] K. Jankowski and J. Paldus, Applicability of coupled-pair theories to quasidegenerate electronic states: A model study, Int. J. Quantum Chem. 18, 1243 (1980).
- [54] J. Paldus, P. Piecuch, L. Pylypow, and B. Jeziorski, Application of Hilbert-space coupled-cluster theory to simple (H₂)₂ model systems: Planar models, Phys. Rev. A **47**, 2738 (1993).
- [55] K. Kowalski and K. Jankowski, Towards Complete Solutions to Systems of Nonlinear Equations of Many-Electron Theories, Phys. Rev. Lett. **81**, 1195 (1998).
- [56] H. L. Tang, V. O. Shkolnikov, G. S. Barron, H. R. Grimsley, N. J. Mayhall, E. Barnes, and S. E. Economou, qubitadapt-VQE: An adaptive algorithm for constructing hardwareefficient Ansätze on a quantum processor, PRX Quantum 2, 020310 (2021).
- [57] W. J. Hehre, R. F. Stewart, and J. A. Pople, self-consistent molecular-orbital methods. I. Use of Gaussian expansions of Slater-type atomic orbitals, J. Chem. Phys. **51**, 2657 (1969).
- [58] D. J. Thouless, Stability conditions and nuclear rotations in the Hartree-Fock theory, Nucl. Phys. **21**, 225 (1960).
- [59] J. Čížek and J. Paldus, Stability conditions for the solutions of the Hartree-Fock equations for atomic and molecular systems. Application to the pi-electron model of cyclic polyenes, J. Chem. Phys. 47, 3976 (1967).
- [60] R. Seeger and J. A. Pople, Self-consistent molecular orbital methods. XVIII. Constraints and stability in Hartree–Fock theory, J. Chem. Phys. 66, 3045 (1977).
- [61] Qiskit contributors, Qiskit: An Open-source Framework for Quantum Computing (2023), doi:10.5281/zenodo.2573505.

- [62] A. M. Childs and N. Wiebe, Hamiltonian simulation using linear combinations of unitary operations, Quantum Inf. Comput. 12, 901 (2012).
- [63] G. Brassard, P. Hoyer, M. Mosca, and A. Tapp, Quantum amplitude amplification and estimation, in *Quantum Computation and Quantum Information*, edited by S. J. Lomonaco, Jr. (AMS Contemporary Mathematics, Washington, D.C., 2002), Vol. 305, pp. 53–74.
- [64] D. W. Berry, A. M. Childs, R. Cleve, R. Kothari, and R. D. Somma, Simulating Hamiltonian Dynamics with a Truncated Taylor Series, Phys. Rev. Lett. 114, 090502 (2015).
- [65] G. H. Low and I. L. Chuang, Optimal Hamiltonian Simulation by Quantum Signal Processing, Phys. Rev. Lett. 118, 010501 (2017).
- [66] A. Gilyén, Y. Su, G. H. Low, and N. Wiebe, Quantum singular value transformation and beyond: Exponential improvements for quantum matrix arithmetics, in *Proceedings of* the 51st Annual ACM SIGACT Symposium on Theory of Computing, STOC 2019 (Association for Computing Machinery, New York, 2019), pp. 193–204.
- [67] V. Verteletskyi, T.-C. Yen, and A. F. Izmaylov, Measurement optimization in the variational quantum eigensolver using a minimum clique cover, J. Chem. Phys. 152, 124114 (2020).
- [68] B. Peng and K. Kowalski, Mapping renormalized coupled cluster methods to quantum computers through a compact unitary representation of non-unitary operators, Phys. Rev. Res. 4, 043172 (2022).
- [69] J. F. Gonthier, M. D. Radin, C. Buda, E. J. Doskocil, C. M. Abuan, and J. Romero, Identifying challenges towards practical quantum advantage through resource estimation: The measurement roadblock in the variational quantum eigensolver, Phys. Rev. Res. 4, 033154 (2022).
- [70] N. C. Rubin, R. Babbush, and M. J., Application of fermionic marginal constraints to hybrid quantum algorithms, New J. Phys. 20, 053020 (2018).
- [71] V. von Burg, G. H. Low, T. Häner, D. S. Steiger, M. Reiher, M. Roetteler, and M. Troyer, Quantum computing enhanced computational catalysis, Phys. Rev. Res. 3, 033055 (2021).
- [72] H. Y. Huang, R. Kueng, and J. Preskill, Predicting many properties of a quantum system from very few measurements, Nat. Phys. **16**, 1050 (2020).
- [73] H.-Y. Huang, R. Kueng, and J. Preskill, Efficient Estimation of Pauli Observables by Derandomization, Phys. Rev. Lett. 127, 030503 (2021).
- [74] S. Aaronson, Shadow tomography of quantum states, in Proceedings of the 50th Annual ACM SIGACT Symposium on Theory of Computing, STOC 2018 (Association for Computing Machinery, New York, 2018), pp. 325–338.
- [75] G. I. Struchalin, Y. A. Zagorovskii, E. V. Kovlakov, S. S. Straupe, and S. P. Kulik, Experimental estimation of quantum state properties from classical shadows, PRX Quantum 2, 010307 (2021).
- [76] S. Chen, W. Yu, P. Zeng, and S. T. Flammia, Robust shadow estimation, PRX Quantum 2, 030348 (2021).
- [77] A. Zhao, N. C. Rubin, and A. Miyake, Fermionic Partial Tomography via Classical Shadows, Phys. Rev. Lett. 127, 110504 (2021).
- [78] A. Acharya, S. Saha, and A. M. Sengupta, Informationally complete POVM-based shadow tomography, arXiv:2105.05992 (2021).

- [79] C. Hadfield, Adaptive pauli shadows for energy estimation, arXiv:2105.12207 (2021).
- [80] S. Hillmich, C. Hadfield, R. Raymond, A. Mezzacapo, and R. Wille, Decision diagrams for quantum measurements with shallow circuits, 2021 IEEE International Conference on Quantum Computing and Engineering (QCE) (IEEE, Piscataway, NJ, 2021), pp. 24-34.
- [81] T. Zhang, J. Sun, X.-X. Fang, X. Zhang, X. Yuan, and H. Lu, Experimental Quantum State Measurement with Classical Shadows, Phys. Rev. Lett. 127, 200501 (2021).
- [82] G. L. Malli, Relativistic and Electron Correlation Effects in Molecules and Solids, NATO ASI Series (Springer Science & Business Media, 2013), Vol. 318.
- [83] H. F. Schaefer, Methods of Electronic Structure Theory, Modern Theoretical Chemistry (Springer Science & Business Media, 2013), Vol. 3.
- [84] G. D. Purvis and R. J. Bartlett, A full coupled-cluster singles and doubles model: The inclusion of disconnected triples, J. Chem. Phys. **76**, 1910 (1982).
- [85] R. J. Bartlett and M. Musiał, Coupled-cluster theory in quantum chemistry, Rev. Mod. Phys. 79, 291 (2007).
- [86] J. Geertsen, M. Rittby, and R. J. Bartlett, The equation-of-motion coupled-cluster method: Excitation energies of Be and Co, Chem. Phys. Lett. 164, 57 (1989).
- [87] D. C. Comeau and R. J. Bartlett, The equation-of-motion coupled-cluster method. Applications to open- and closed-shell reference states, Chem. Phys. Lett. 207, 414 (1993).
- [88] K. W. Schmid, On the use of general symmetry-projected Hartree–Fock–Bogoliubov configurations in variational approaches to the nuclear many-body problem, Prog. Part. Nucl. Phys. 52, 565 (2004).
- [89] N. Tomita, Many-body wave functions approximated by the superposition of spin-projected nonorthogonal slater determinants in the resonating Hartree-Fock method, Phys. Rev. B **69**, 045110 (2004).
- [90] C. A. Jiménez-Hoyos, T. M. Henderson, T. Tsuchimochi, and G. E. Scuseria, Projected Hartree–Fock theory, J. Chem. Phys. **136**, 164109 (2012).
- [91] R. Rodríguez-Guzmán, K. W. Schmid, C. A. Jiménez-Hoyos, and G. E. Scuseria, Symmetry-projected variational approach for ground and excited states of the two-dimensional Hubbard model, Phys. Rev. B 85, 245130 (2012).
- [92] C. A. Jiménez-Hoyos, R. Rodríguez-Guzmán, and G. E. Scuseria, Excited electronic states from a variational approach based on symmetry-projected Hartree–Fock configurations, J. Chem. Phys. 139, 224110 (2013).
- [93] R. Rodríguez-Guzmán, C. A. Jiménez-Hoyos, R. Schutski, and G. E. Scuseria, Multireference symmetry-projected variational approaches for ground and excited states of the one-dimensional Hubbard model, Phys. Rev. B 87, 235129 (2013).
- [94] I. Theophilou, M. Tassi, and S. Thanos, Charge transfer excitations from excited state Hartree-Fock subsequent minimization scheme, J. Chem. Phys. 140, 164102 (2014).
- [95] N. P. Bauman, E. J. Bylaska, S. Krishnamoorthy, G. H. Low, N. Wiebe, C. E. Granade, M. Roetteler, M. Troyer, and K. Kowalski, Downfolding of many-body Hamiltonians using

- active-space models: Extension of the subsystem embedding subalgebras approach to unitary coupled cluster formalisms, J. Chem. Phys. **151**, 014107 (2019).
- [96] K. Kowalski and N. P. Bauman, Sub-system quantum dynamics using coupled cluster downfolding techniques, J. Chem. Phys. **152**, 244127 (2020).
- [97] N. P. Bauman and K. Kowalski, Coupled cluster down-folding theory: Towards universal many-body algorithms for dimensionality reduction of composite quantum systems in chemistry and materials science, Materials Theory 6, 17 (2022).
- [98] M. Zheng, B. Peng, N. Wiebe, A. Li, X. Yang, and K. Kowalski, QuGCM, https://github.com/pnnl/QuGCM (2022).

- [99] D. J. Thouless, The Quantum Mechanics of Many-Body Systems (Courier Corporation, 2014).
- [100] J. Paldus and J. Čĺžzek, Stability conditions for the solutions of the Hartree–Fock equations for atomic and molecular systems. II. Simple open-shell case, J. Chem. Phys. 52, 2919 (1970).
- [101] X. Li and J. Paldus, Do independent-particle-model brokensymmetry solutions contain more physics than the symmetryadapted ones? The case of homonuclear diatomics, J. Chem. Phys. **130**, 084110 (2009).
- [102] D. An and L. Lin, Quantum linear system solver based on time-optimal adiabatic quantum computing and quantum approximate optimization algorithm, ACM Trans. Quantum Comput. 3, 1 (2022).